COMPUTATIONAL MODELLING OF CRACKS IN VISCOPLASTIC MEDIA

G.N. Wells*, L.J. Sluys and R. de Borst

Koiter Institute Delft
Delft University of Technology
P.O. Box 5048, 2600 GA Delft, The Netherlands

ABSTRACT

A newly developed numerical model is used to simulate propagating cracks in a strain softening viscoplastic medium. The model allows the simulation of displacement discontinuities independently of a finite element mesh. This is possible using the partition of unity concept, in which fracture is treated as a coupled problem, with separate variational equations corresponding to the continuous and discontinuous parts of the displacement field. The equations are coupled through the dependence of the stress field on the strain state. Numerical examples show that allowing displacement discontinuities in a viscoplastic Von Mises material can lead to a failure mode that differs from a continuum-only model.

KEYWORDS

Displacement discontinuity, viscoplasticity, strain softening.

INTRODUCTION

Two distinct stages can be identified in the failure of quasi-brittle and ductile materials. The first stage involves the localisation of inelastic deformations into narrow zones. Later in the loading process, macroscopic displacement discontinuities across surfaces can be identified. Depending on the ductility of the material, this occurs at a point between the peak load and complete global failure. Computationally, failure is usually simulated using a continuum (regularised strain softening) or a discontinuous (cohesive zone, LEFM) model. Continuum models are well suited for modelling the inelastic deformations that develop early in the loading process, but are unable to represent the free surfaces that develop in a body prior to complete failure. Discontinuous models are well-suited for highly localised failure, but less adept at representing the distributed inelastic deformations near the peak load in quasi-brittle materials and the substantial plastic flow that occurs during the failure of ductile materials. A model is presented which is able to capture both stages of the failure process. Initial inelastic deformations are represented in the continuum using a regularised strain softening model, and the later development of discrete surfaces within a body is simulated by inserting a displacement discontinuity.

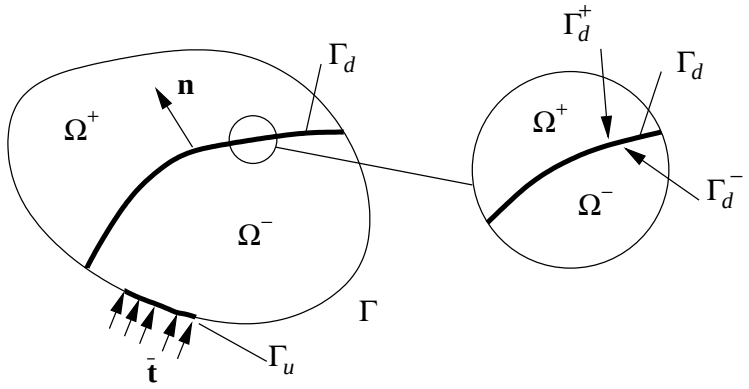

Figure 1: Body Ω crossed by a single discontinuity Γ_d.

To simulate strain softening in the continuum, a regularised continuum model must be used. In this work, a Perzyna viscoplastic model is used [1]. When the inelastic deformation at the tip of a discontinuity reaches a critical level, the discontinuity is extended. A displacement discontinuity is added to the underlying finite element interpolation basis using the partition of unity concept [2, 3]. Using the partition of unity concept, a displacement discontinuity can be modelled by adding extra degrees of freedom to existing nodes. The displacement field is decomposed into a continuous and a discontinuous part, with 'regular' nodal degrees of freedom representing the continuous part of the displacement field and 'enhanced' nodal degrees of freedom representing the discontinuous part of the displacement field. This method has been used successfully for simulating cracks in elastic bodies [4] and cohesive cracks under both static [5] and impact [6] loading.

To elaborate the model, the kinematics of a body crossed by a displacement discontinuity are first discussed. Aspects of introducing a displacement discontinuity in an inelastic continuum are then considered and the model is demonstrated through several numerical examples. The numerical examples highlight the influence of including a displacement discontinuity on the failure mode for a Von Mises material.

INCLUDING A DISPLACEMENT DISCONTINUITY

The proposed formulation allows a displacement discontinuity to be added to a finite element model, independently of the spatial discretisation. Rather than explicitly modelling a discontinuity through the mesh structure, a displacement jump is described mathematically using the Heaviside function.

Discontinuous displacement field

The displacement field $\mathbf{u}$ for a body crossed by multiple, non-intersecting displacement discontinuities can be described by:

$$\mathbf{u}(\mathbf{x},t) = \hat{\mathbf{u}}(\mathbf{x},t) + \sum_{i=1}^{k} \mathscr{H}_{\Gamma_{d,i}}(\mathbf{x})\tilde{\mathbf{u}}_i(\mathbf{x},t) \tag{1}$$

where $\hat{\mathbf{u}}$ and $\tilde{\mathbf{u}}_i$ are continuous functions, $\mathscr{H}_{\Gamma_{d,i}}$ is the Heaviside function centred at the ith discontinuity and k is the number of discontinuities. A body, crossed by a single discontinuity is shown in figure 1. The Heaviside jump is defined as $\mathscr{H}_{\Gamma_d}(\mathbf{x}) = 1,\ \mathbf{x} \in \Omega^+$ and $\mathscr{H}_{\Gamma_d}(\mathbf{x}) = 0,\ \mathbf{x} \in \Omega^-$, where the domains Ω^+ and Ω^- are shown in figure 1. The magnitude of the displacement jump at the ith discontinuity $[\![\mathbf{u}]\!]_i$ is given by $\tilde{\mathbf{u}}_{i,\mathbf{x}\in\Gamma_{d,i}}$. Taking

the symmetric gradient of equation (1), the strain field for the geometrically linear case is given by:

$$\boldsymbol{\varepsilon} = \boldsymbol{\nabla}^{\mathrm{S}}\mathbf{u} = \boldsymbol{\nabla}^{\mathrm{S}}\hat{\mathbf{u}} + \sum_{i=1}^{k} \mathscr{H}_{\Gamma_{d,i}} \left(\boldsymbol{\nabla}^{\mathrm{S}}\tilde{\mathbf{u}}_i\right) + \sum_{i=1}^{k} \delta_{\Gamma_d,i} \left(\tilde{\mathbf{u}}_i \otimes \mathbf{n}_i\right)^{\mathrm{S}} \tag{2}$$

with $\delta_{\Gamma_d,i}$ the Dirac-delta distribution centred at the *i*th displacement discontinuity and **n** is the normal vector to the discontinuity.

Variational formulation

The proposed model can be interpreted as a coupled problem, with one equation describing the continuous part of the displacement field, $\hat{\mathbf{u}}$, and a second describing the discontinuous part of the displacement field, $\mathscr{H}_{\Gamma_d}\tilde{\mathbf{u}}$. Following a Galerkin procedure, the weak governing equations can be formed by inserting the displacement decomposition in equation (1) into the virtual work equation. After some manipulations, two weak governing equations can be formed for a body crossed by a single discontinuity [5]:

$$\begin{aligned} &\int_{\Omega} \boldsymbol{\nabla}^{\mathrm{S}}\hat{\boldsymbol{\eta}} : \boldsymbol{\sigma} = \int_{\Gamma_u} \hat{\boldsymbol{\eta}} \cdot \bar{\mathbf{t}}\, d\Gamma \\ &\int_{\Omega^+} \boldsymbol{\nabla}^{\mathrm{S}}\tilde{\boldsymbol{\eta}} : \boldsymbol{\sigma} + \int_{\Gamma_d} \tilde{\boldsymbol{\eta}} \cdot \mathbf{t} = \mathscr{H}_{\Gamma_u} \int_{\Gamma_d} \tilde{\boldsymbol{\eta}} \cdot \bar{\mathbf{t}}\, d\Gamma \end{aligned} \tag{3}$$

where $\hat{\boldsymbol{\eta}}$ and $\tilde{\boldsymbol{\eta}}$ are admissible displacement variations, **t** is the traction acting at a discontinuity Γ_d and $\bar{\mathbf{t}}$ are tractions acting on the external boundary Γ_u. The unbounded Dirac-delta term has been eliminated by changing the volume integral containing the distribution to a surface integral over Γ_d.

Finite element implementation

The weak governing equations in equation (3) are solved in a similar manner to a coupled problem. Different sets of nodal degrees of freedom are used to represent the continuous and the discontinuous parts of the displacement field. In a discretised format, the displacement field is given by:

$$\mathbf{u} = \underbrace{\mathbf{Na}}_{\hat{\mathbf{u}}} + \mathscr{H}_{\Gamma_d} \underbrace{\mathbf{Nb}}_{\tilde{\mathbf{u}}} \tag{4}$$

where **N** is the standard matrix containing the element shape functions and the vectors **a** and **b** relate to the continuous and discontinuous parts of the displacement field, respectively. The discretised weak governing equations are formed by inserting the discretised displacement field in equation (4) and its gradient into equation (3).

The extra **b** degrees of freedom are added only to nodes close to a discontinuity. If the support of a node is crossed by a discontinuity, the **b** degrees of freedom are activated to describe the discontinuity. The addition of extra degrees of freedom to nodes whose support is not crossed by a discontinuity leads to a global stiffness matrix which is not positive definite since over the support of the node the Heaviside function is equivalent to a constant function, which is included in the span of the standard shape functions.

SIMULATING THE CONTINUUM-DISCONTINUOUS TRANSITION

A displacement discontinuity is extended when the inelastic deformation in the continuum at a discontinuity tip reaches a critical level. For the Perzyna viscoplastic model, a discontinuity is extended when the yield

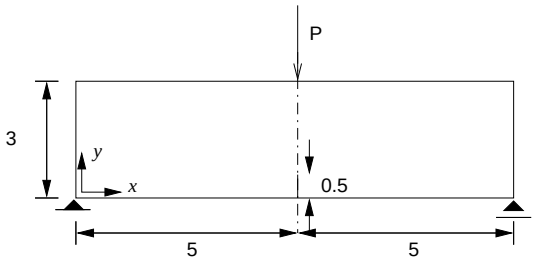

Figure 2: Three-point bending beam. All dimensions in millimetres (depth = 1mm).

strength of the underlying rate-independent model is exhausted. At this stage, the material is considered to have lost all coherence. Therefore, no tractions can be transmitted across an opening discontinuity. Since the rate-dependent constitutive model remains well-posed, it is not possible to draw on linear stability analysis to determine a discontinuity propagation direction. Therefore, a discontinuity is assumed to extend in the direction in which the effective stress is maximum. This is determined by a spatial weighting procedure around a discontinuity tip [7, 8]. Using an effective stress to determine the propagation direction is dependent on the chosen yield function and makes the procedure equally applicable to both mode-I and mode-II failure problems [8].

NUMERICAL EXAMPLES

To illustrate the combined continuum-discontinuous model, a three-point bending test (figure 2) is performed for a Von Mises material. A discontinuity propagates from a 0.5 mm long initial cut at the centre of the beam at the bottom edge. The material properties are initially taken as: Young's modulus $E = 1 \times 10^2$ MPa, Poisson's ratio $\nu = 0.2$, yield stress $\bar{\sigma} = 1$ MPa, viscosity $\eta = 2$ s and the hardening modulus $h = -200$ Nmm^{-2}. The beam is loaded via a constant downward velocity of 1 mms^{-1}, applied at the centre of the beam on the top edge. The analyses are performed under plane strain conditions and the six-noded triangle is used as the underlying finite element.

To illustrate the objectivity of the model with respect to finite element mesh structure, the beam is analysed using two different meshes. The first is a structured mesh composed of 4750 elements and the second is an unstructured mesh composed of 3631 elements. Figure 3 shows the equivalent plastic strain field and the discontinuity path for the two meshes near complete failure. The size and shape of the plastic zones are the same and a discontinuity has propagated through the beam towards the loading point. To examine more closely the failure mode, the evolution of the equivalent plastic strain field and displacement discontinuity are shown in figure 4. The failure mode is clearly mode-I dominated. A discontinuity propagates through the beam, with a plastic hinge forming only at the last stage of failure.

To highlight the influence of including a displacement discontinuity, the three-point bending test is re-analysed with an initial discontinuity which is not allowed to extend. The equivalent plastic strain field for this case is shown in figure 5. The failure mode differs fundamentally from the case of a propagating discontinuity. The beam has failed through the development of a plastic hinge, with the centre of the beam remaining elastic. The difference in response is due to the plastic incompressibility constraint for the continuum plasticity model. The introduction of a discontinuity implies the complete failure of the material and therefore no volumetric constraint can exist, making mode-I opening possible.

The three-point bending test is again analysed for a propagating discontinuity, but now for an increased hardening modulus of $h = -20$ Nmm^{-2}, ten times greater than for the previous example. The evolution of the equivalent plastic strain and the displacement discontinuity for this case are shown in figure 6. The failure

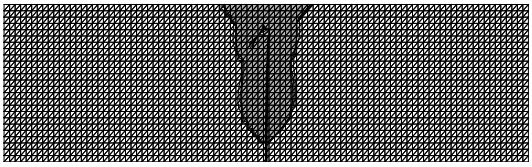

(a)

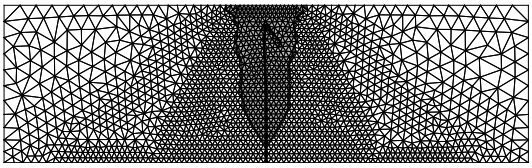

(b)

Figure 3: Equivalent plastic strain contours and discontinuity path for three-point bending test under plane strain conditions at $u = -0.4$ mm with (a) structured and (b) unstructured meshes.

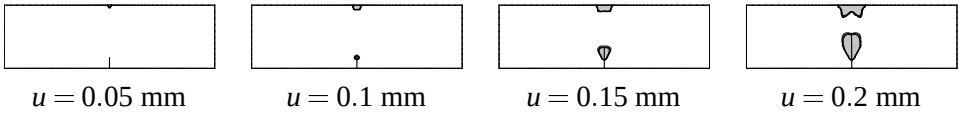

$u = 0.05$ mm $u = 0.1$ mm $u = 0.15$ mm $u = 0.2$ mm

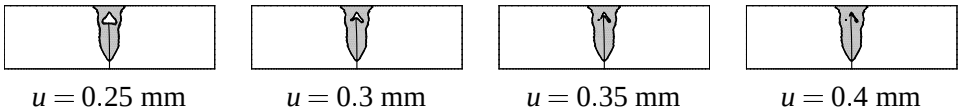

$u = 0.25$ mm $u = 0.3$ mm $u = 0.35$ mm $u = 0.4$ mm

Figure 4: Evolution of equivalent plastic strain contours and discontinuity for the three-point bending test under plane strain conditions.

mode for this example is different than that for the more brittle beam in figure 4. Rather than mode-I, the failure mode of the ductile beam is mode-II. The discontinuity has extended over only a short distance and a plastic hinge has formed. This example shows that when a discontinuity is introduced, for a Von Mises material the hardening modulus influences the failure mode.

CONCLUSIONS

Numerical examples have been presented which show the influence of including a propagating displacement discontinuity when simulating failure in a Von Mises material. The inclusion of a displacement discontinuity allows cleavage opening modes which are restrained by a continuum-only model through the plastic incompressibility constraint. The inclusion of a discontinuity makes mode-I dominated failure possible when using

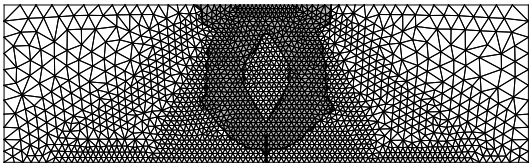

Figure 5: Equivalent plastic strain contours for a stationary discontinuity at $u = 1$ mm for the Von Mises yield surface.

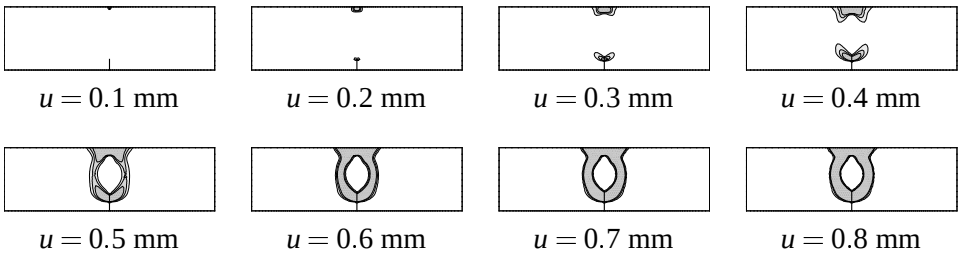

Figure 6: Evolution of equivalent plastic strain contours and discontinuity for the three-point bending test under plane strain conditions for a ductile beam. The hardening modulus h is equal to -20 Nmm^{-2}.

a continuum model that obeys a Von Mises flow rule.

ACKNOWLEDGEMENTS

This research is supported by the Technology Foundation STW, applied science division of NWO and the technology program of the Ministry of Economic Affairs and the Ministry of Public Works and Water Management, The Netherlands.

REFERENCES

1. Perzyna, P. (1966). Fundamental problems in viscoplasticity. In: *Recent Advances in Applied Mechanics*, volume 9, pp. 243–377. Academic Press, New York.

2. Babuška, I. and Melenk, J. M. (1997). The Partition of Unity Method. *International Journal for Numerical Methods in Engineering*, 40(4), 727–758.

3. Duarte, C. A. and Oden, J. T. (1996). H-p clouds – an h-p meshless method. *Numerical Methods for Partial Differential Equations*, 12(6), 673–705.

4. Belytschko, T. and Black, T. (1999). Elastic crack growth in finite elements with minimal remeshing. *International Journal for Numerical Methods in Engineering*, 45(5), 601–620.

5. Wells, G. N. and Sluys, L. J. (2001). A new method for modelling cohesive cracks using finite elements. *International Journal for Numerical Methods in Engineering*, 50(12), 2667–2682.

6. Wells, G. N. and Sluys, L. J. (2001). Discontinuous analysis of softening solids under impact loading. *International Journal for Numerical and Analytical Methods in Geomechanics*, 25(7), 691–709.

7. Wells, G. N., De Borst, R. and Sluys, L. J. (2001). An enhanced finite element method for analysing failure in elasto-plastic solids. In: *Trends in Computational Structural Mechanics* (CDROM), Wall, W. A., Bletzinger, K. U. and Schweizerhof, K., eds., pp. 397–406. CIMNE, Barcelona, Spain.

8. Wells, G. N., Sluys, L. J. and De Borst, R. (2001). Simulating the propagation of displacement discontinuities in a regularised strain-softening medium. *International Journal for Numerical Methods in Engineering*. (accepted).